Saikosaponin b2 inhibits tumor angiogenesis in liver cancer via down-regulation of VEGF/ERK/HIF-1α signaling

MAN YOU[1,2*], JUNMIN FU[1,3*], XINGZHI LV[1], LAN WANG[1], HONGWEI WANG[1] and RUIFANG LI[1]

[1]Department of Pharmacology, Medical College, Henan University of Science and Technology; [2]Department of Pharmacy, Luoyang Orthopedic-Traumatological Hospital of Henan Province (Henan Provincial Orthopedic Hospital), Luoyang, Henan 471000; [3]Department of Pharmacy, Henan University of Chinese Medicine, Zhengzhou, Henan 450046, P.R. China

Received August 30, 2022; Accepted January 20, 2023

DOI: 10.3892/or.2023.8573

Abstract. Saikosaponin b2 (SSb2) is an active component of Radix Bupleuri, which is commonly used in traditional Chinese medicine for defervescence and liver protection. In the present study, it was demonstrated that SSb2 exhibited potent antitumor activity by inhibiting tumor angiogenesis *in vivo* and *in vitro*. As measured by tumor weight and measures of immune function such as thymus index, spleen index and white blood cell count, SSb2 inhibited tumor growth, with low immunotoxicity, in H22 tumor-bearing mice. Furthermore, proliferation and migration of HepG2 liver cancer cells was inhibited following SSb2 treatment, which demonstrated SSb2's antitumor effect. The angiogenesis marker CD34 was downregulated in the SSb2-treated tumor samples, which suggested the antiangiogenic activity of SSb2. Furthermore, the chick chorioallantoic membrane assay demonstrated the potent inhibitory effect of SSb2 on basic fibroblast growth factor-induced angiogenesis. *In vitro*, SSb2 significantly inhibited numerous stages of angiogenesis, including the proliferation, migration and invasion of human umbilical vein endothelial cells. Further mechanistic studies demonstrated that SSb2 treatment reduced the levels of key proteins involved in angiogenesis, including vascular endothelial growth factor (VEGF), phosphorylated ERK1/2, hypoxia-inducible factor (HIF)-1α, MMP2 and MMP9 in H22 tumor-bearing mice, which supported the HepG2 liver cancer cell results. Overall, SSb2 effectively inhibited angiogenesis via the VEGF/ERK/HIF-1α signal pathway and may serve as a promising natural agent for liver cancer treatment.

Correspondence to: Professor Ruifang Li, Department of Pharmacology Medical College, Henan University of Science and Technology, 263 Kai Yuan Road, Luoyang, Henan 471000, P.R. China
E-mail: ylliruifang@163.com

*Contributed equally

Key words: Saikosaponin b2, liver cancer, angiogenesis, vascular endothelial growth factor

Introduction

Liver cancer is the fifth most prevalent cancer and the second most common cause of tumor-related deaths worldwide (1,2). China accounts for approximately 50% of the world's new cases and deaths regarding this disease (3). The main etiological factors of liver cancer include hepatitis B virus, hepatitis C virus, aflatoxin contamination and alcoholic liver disease. The current clinical treatment of liver cancer is lacking due to the low curative ratio and high recurrence rate. Despite their importance as a treatment method, chemotherapeutic drugs have numerous serious side effects; therefore, developing natural agents with improved therapeutic efficacy and low toxicity, to combat liver cancer, is essential.

Saikosaponin (SS) is the main active component of Radix Bupleuri, accounting for ~7% of the total dry weight of the roots of *Bupleurum chinense* DC. It possesses many important pharmacological activities, including immune regulation (4), liver protection (5), liver fibrosis inhibition as well as anti-inflammatory (6), antiviral (7) and antitumor (8) activities. SS's antitumor activity regulates fundamental cellular processes, such as S-phase DNA synthesis, protein metabolism, proliferation and apoptosis. Several monomers have been identified in SS, including SSa, SSb1, SSb2, SSc, SSd and SSe, based on their different chemical structures. Numerous studies have demonstrated that SSa and SSd have potent antitumor effects (8). However, little is known about SSb2's effect on liver protection and cancer prevention. We previously demonstrated that SSb2 significantly mitigated LPS/GalN-induced acute liver injury in mice. This effect may be attributable to decreased NF-κB and increased Sirt-6 protein expression levels, both of which improve inflammatory injury and energy metabolism (9). Further study on SSb2's role in liver cancer is crucial for the development of safe and effective new anticancer agents.

Liver cancer is a highly vascularized solid tumor in which the growth of new blood vessels continuously supplies oxygen and nutrients to tumor cells (10). As a prerequisite for continued tumor growth, angiogenesis significantly contributes to liver cancer development. Recent cancer research studies have concentrated on anti-angiogenesis as a novel approach for the treatment of cancers with poor prognoses (11,12). Antiangiogenic therapy has become an important adjunct

to conventional chemotherapy in the treatment of many solid tumors (13,14). The vascular endothelial growth factor (VEGF) is a key regulator of angiogenesis and its expression is closely associated with liver cancer (15). In most experimental systems, hypoxia-inducible factor-1α (HIF-1α) regulates VEGF transcription (10,16). HIF-1α is closely associated with important aspects of tumor biology, such as angiogenesis, invasion, glucose metabolism and cell survival, and it is overexpressed in many human cancers (17). Notably, VEGF/HIF-1α is the target of many anti-liver cancer drugs, which are considered a promising treatment strategy for liver cancer (18-20). The present study evaluated the role of SSb2 in liver cancer to determine whether SSb2 suppresses liver cancer development through regulation of the expression of proteins involved in angiogenic pathways.

Materials and methods

Materials and reagents. SSb2 was purchased from Chengdu Must Bio-Technology Co., Ltd. Doxorubicin (DOX) was purchased from Haizheng Pharmaceutical Co., Ltd. Dulbecco's modified eagle medium (DMEM) was purchased from Gibco (Thermo Fisher Scientific, Inc.). Trypase and methylthiazolyl tetrazolium bromide (MTT) were purchased from MilliporeSigma. The BCA Protein Assay Kit and Super Signal West Pico Chemiluminescent Substrate were purchased from Pierce (Thermo Fisher Scientific, Inc.). Radioimmunoprecipitation assay (RIPA) Lysis Buffer and 10x poly-L-lysine were purchased from Beijing Solarbio Science & Technology Co., Ltd. Antibodies against CD34 (1:10,000, cat. no. 60180-1-Ig), VEGF (1:500, cat. no. 19003-1-AP), MMP9 (1:500, cat. no. 10375-2-AP) and β-actin (1:1,000, cat. no. CL594-66009) were purchased from Wuhan Sanying Biotechnology; antibodies against MMP2 (1:500, cat. no. TA806846) and ERK1/2 (1:500, cat. no. TA325139) were purchased from Origene Technologies, Inc.; and antibodies against p-ERK1/2 (1:500, cat. no. sc-7383), mouse anti-rabbit IgG-HRP (1:1,000, cat. no. sc-2357) and goat anti-mouse IgG-HRP (1:1,000, cat. no. sc-2005) were purchased from Santa Cruz Biotechnology, Inc.

Animals and ethics statement. A total of 50 Male Balb/c mice weighing 18-22 g were purchased from the Experimental Animal Center of The Medical College of Henan University of Science and Technology. The Experimental Animal Ethics Committee of Henan University of Science and Technology approved the experimental protocols involving animals and fertilized chicken eggs (approval no. 20200519). All animal experiments were performed according to The National Act on the Use of Experimental Animals (China). Appropriate measures were taken to minimize the use and suffering of animals.

Cell culture. The human liver cancer cell line HepG2 was purchased from the Shanghai Institutes for Biological Sciences (cat. no. SNL-083). Human umbilical vein endothelial cells (HUVECs) were purchased from Procell Life Science & Technology Co., Ltd.(cat. no. CL-0675). H22 liver cancer cells were purchased from the Henan Institute of Medical Sciences (cat. no. CL-0341). The identify of each cell line was confirmed using short tandem repeat profiling analysis. HepG2 and HUVECs were cultured in high-glucose DMEM (Gibco; Thermo Fisher Scientific, Inc.) and H22 cells were cultured in Roswell Park Memorial Institute 1640 medium (Gibco; Thermo Fisher Scientific, Inc) both supplemented with 10% fetal bovine serum (FBS) (Gibco; Thermo Fisher Scientific, Inc.). All cells were incubated at 37˚C in a 5% CO_2, humidified atmosphere.

Cell viability assay. HepG2 liver cancer cells and HUVECs were seeded at a density of $2.5x10^4$ cells/well in 96-well plates for 24 h at 37˚C in a 5% CO_2 incubator before treatment with different SSb2 concentrations at 37˚C. After 20 h of culturing with SSb2, 20 μl MTT (5 mg/ml) was added to each well, followed by incubation for 4 h at 37˚C. Then, 200 μl dimethyl sulfoxide was added to each well after removing the supernatant. The final absorbance was measured at a wavelength of 490 nm using a microplate reader.

H22 liver cancer transplanted tumor model. Mice were housed in a sterile environment at 22±1˚C, a relative humidity of 40-70% and a 12 h light/dark cycle. The mice had free access to rodent chow and drinkable water. The H22 model was established through subcutaneous injection, as described previously (21,22). The suspension of H22 liver cancer cells was adjusted to a density of $1x10^6$/ml, and 0.2 ml of H22 liver cancer cell suspensions were subcutaneously inoculated into the right armpit region of each mouse. After 24 h, the mice were randomly divided into 5 groups (n=10) as follows: The control group [normal saline, intraperitoneal (i.p.) injection, once a day], SSb2-low, middle and high dose groups (5, 10 and 20 mg/kg/day, respectively, i.p. injection, once a day) and the positive control group (DOX, 2 mg/kg/day, i.p. injection, once every two days). All animals were treated for 10 days. The mice's health and behavior were monitored and recorded daily. On the 10th day, blood samples were collected to perform a white blood cell count using a cell counting plate. Isoflurane was administered via inhalation as anesthesia with an induction concentration of 4-5% and a maintenance concentration of 2-3%. At the study endpoint all mice were euthanized by cervical dislocation under anesthesia. Humane endpoints were identified as xenograft tumor diameter >20 mm, the xenograft tumor weight >10% of the animal's body weight, body weight loss due to tumor growth >20% of the animal's body weight, or an animal was deemed to be in poor health and did not eat. Observations of pupil dilation and cessation of heartbeat and breath were used to confirm the animal's death. Following euthanasia, the tumors were carefully isolated and processed for further analysis. Tumor tissues, the thymus and the spleen were collected and weighed in order to calculate the tumor inhibitory rate and organ index, as follows: Tumor growth inhibition rate (%)=1-(tumor weight in SSb2 or DOX group/tumor weight in control group) x100; and organ index=organ weight (mg)/body weight (g).

Hematoxylin and eosin (H&E) staining, CD34 immunostaining and microvessel density (MVD) counting. The tumor tissues were fixed using a 10% formaldehyde solution for 12 h at room temperature, followed by rinsing in running water

for 12 h. The fixed tumor tissues were then dehydrated using increasing ethanol concentrations, embedded in paraffin and sectioned to a 4 μm thickness. The tumor sections were stained using H&E for histologic examination. In this process, the paraffin embedded sections were placed into xylene two successively times for dewaxing, for 15 min each at room temperature. Then the sections were successively placed in 100, 100, 95, 80 and 70% ethanol, and double distilled water, 5 min each at room temperature. The tissue sections were stained with hematoxylin for 2 min and eosin for 1.5 min, both at room temperature. After that, the sections were dehydrated in 70, 80 and 95% ethanol, followed by immersion in absolute ethanol twice and xylene twice for treatment, 3 min each at room temperature. Finally, the sections were sealed using neutral resin. Microscopic images were captured using a light microscope (Olympus Corporation). For immunohistochemistry staining, tumor sections were placed into a 60˚C incubator for 60 min, and then the slides were dewaxed twice in xylene (the first for 30 min and the second for 15 min). Then, the slides were rehydrated using decreasing ethanol concentrations. The slides were then incubated in trypsin solution (trypsin solution:trypsin diluent, 1:3, MilliporeSigma) for 30 min at 37˚C, and then washed in phosphate-buffered saline (PBS) three times. The slides were incubated with 3% H_2O_2 solution for 15 min at room temperature, and after washed three times in PBS, goat serum was used for blocking at 37˚C for 20 min. The primary antibody (anti-CD34 antibody, 1:50, cat. no. 60180-1-Ig, Proteintech Group, Inc.) was added for incubation overnight at 4˚C. After washing three times in PBS, the slides were incubated with secondary antibody (bio-goat anti-mouse IgG, 1:1,000, cat. no. sc-2005, Santa Cruz Biotechnology, Inc) for 20 min at 37˚C. The slides were incubated with streptavidin-peroxidase for 20 min at room temperature after 3 washes with PBS. Finally, diaminobenzidine was used for 4 min at room temperature followed by washing with PBS, and hematoxylin was used for staining for 2 min at room temperature. At last, the slides were dehydrated with ethanol and xylene, and then were covered. The images were obtained using a light microscope (Olympus Corporation). Microvessel density was evaluated using five randomly selected fields of view from each section at 200x magnification. Any single cell or discrete cluster, stained brown, that indicated positive CD34 reactivity was identified as a single countable vessel. The MVD for each case was determined as the mean count of the five fields of view.

Western blotting. Total proteins were extracted from tumor tissues and HepG2 liver cancer cells using RIPA lysis buffer, the concentration of extracted protein was quantified using a bicinchoninic acid (BCA) protein assay kit, and the protein lysates (70 μg/lane) were subjected to 12% SDS-PAGE and transferred onto a nitrocellulose membrane. The membranes were then incubated overnight at 4˚C with primary antibodies after being blocked with 5% non-fat dry milk at 37˚C for 1 h. After three washes with PBST (0.05% Tween-20), membranes were incubated with the aforementioned secondary antibodies for 1 h at room temperature. Signals were assessed using an enhanced chemiluminescence kit (Thermo Fisher Scientific, Inc.) and the gray values were measured by Gel-Pro analyzer 32 (Media Cybernetics. Inc.).

Transwell migration and invasion assay. For the Transwell migration assay, HUVECs were seeded into the upper chamber of the Transwell plate at a density of $3x10^5$ cells/well into wells containing 100 μl serum-free medium. A total of 600 μl HUVEC special medium (cat. no. CM-0122, Procell Life Science & Technology Co., Ltd.) with 20% FBS (Gibco; Thermo Fisher Scientific, Inc.) was added in the bottom chamber as a chemoattractant. After SSb2 (25, 50, 100 μg/ml) treatment, the cells were cultured in a 37˚C incubator for 8 h. HUVECs that migrated to the bottom chamber were fixed using 4% paraformaldehyde at room temperature for 30 min and stained for 30 min using 0.1% crystal violet at room temperature. HUVEC migration was observed and quantified using an inverted light microscope. For the Transwell invasion assay, 50 μl of diluted Matrigel was pre-applied to the upper chamber, then placed in a 37˚C incubator overnight. All other procedures were identical to those for the Transwell migration experiments.

Wound-healing assay. HUVECs and HepG2 liver cancer cells were seeded in 6-well plates and cultured in high-glucose DMEM supplemented with 10% FBS at 37˚C for 24 h (23,24) until the cells were densely confluent (80-90%), after which the monolayer cells were scratched using a sterile 200 μl pipette tip and washed with PBS to remove nonadherent cells. Then the cells were incubated for an additional 24 h (HUVECs) or 48 h (HepG2) in serum-free medium with or without SSb2 (25, 50, 100 μg/ml) treatment., Plates were imaged using an inverted light microscope. The width of the cell-free gap was measured to calculate the migration rate using Image J (version 1.53m, National Institutes of Health).

Chicken embryo chorioallantoic membrane (CAM) assay. For 10 days, fertilized chicken eggs were incubated at 37˚C and 65-70% relative humidity in an incubator. On day 11, a window of approximately 1 cm^2 was gently opened with a tweezer in the chick embryo air sac. The eggs were selected at random and divided into 5 groups (n=10). SSb2 (0.1, 0.2 0.4 μg/embryo) and DOX (0.2 μg/embryo) were injected into the chick embryonic blood vessel branch, the control group were administered the same volume of normal saline.

An additional, 60 chicken embryos were selected and divided into 6 groups (n=10). Groups were treated as above, with an additional group basic fibroblast growth factor (b-FGF) group (0.1 μg/embryo) introduced; the aforementioned SSb2 groups also contained the growth factor b-FGF (0.1 μg/embryo) as an inducer. The windows were then covered with sterile membranes, and the eggs were returned for incubation for an additional 3 days. Subsequently, the CAM microvessels were imaged using a light microscope (Olympus Corporation) after fixation using 4% formaldehyde for 8 h at room temperature. The number of vascular branches were recorded in eight fields of view per embryo and a mean calculated to quantify the effect of SSb2 on angiogenesis.

Statistical analysis. SPSS22.0 (IBM Corp.) was used for statistical analysis. Data were presented as mean ± SD. Comparisons among multiple groups were performed using a one-way analysis of variance followed by Dunnett's or Tukey's post hoc tests. $P<0.05$ was considered to indicate a statistically significant difference.

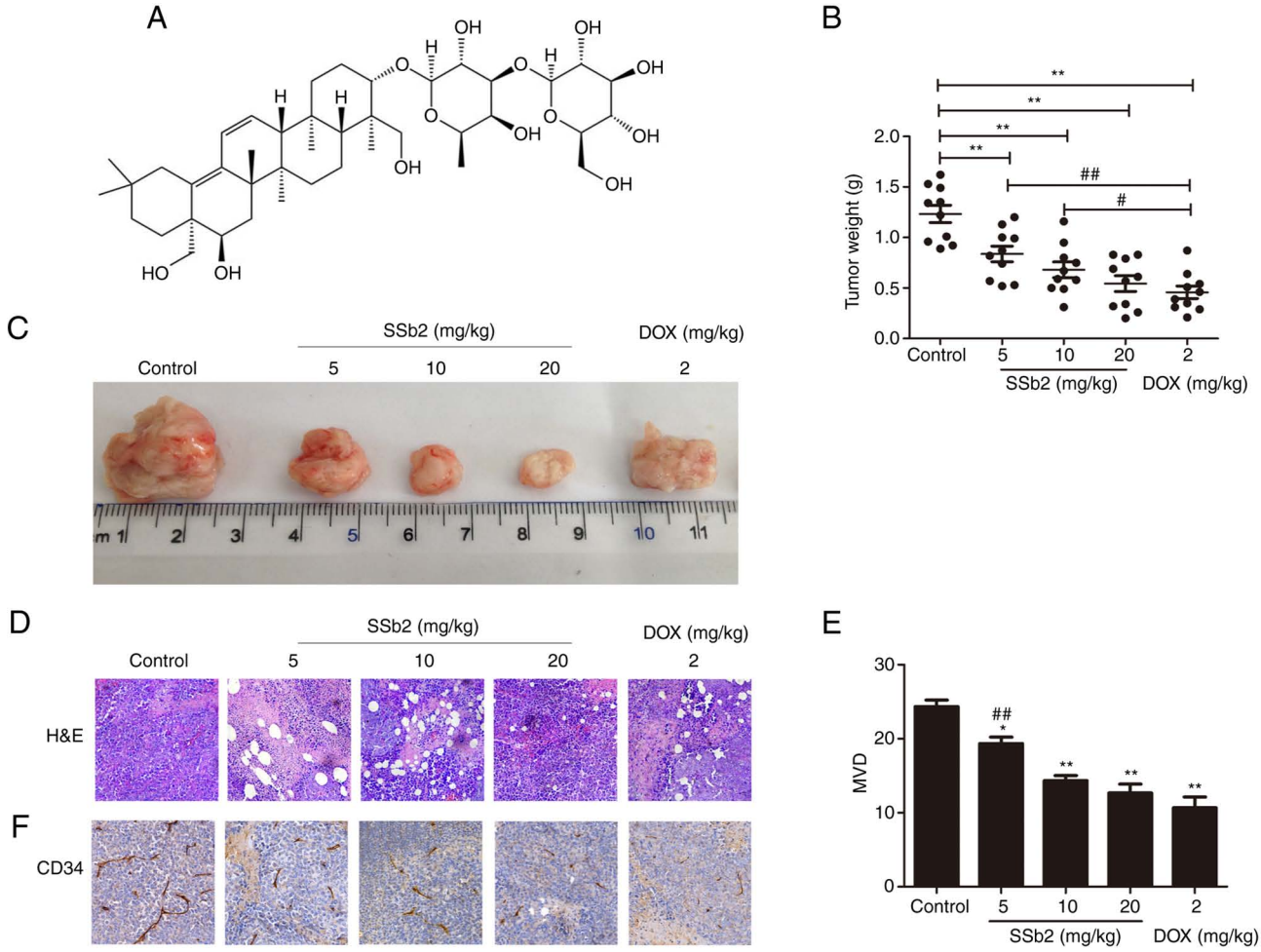

Figure 1. Effects of SSb2 on H22 tumor-bearing mice. (A) Chemical structure of SSb2. (B) Mean tumor weights of mice in different groups. (C) Representative images of xenograft tumors in different groups. (D) Pathomorphological changes in tumor tissue of H22 tumor-bearing mice (H&E staining, magnification, x200). (E). MVD of different groups. (F) Representative images of CD34 immunohistochemical staining of tumor tissues in different groups (magnification, x200) *P<0.05 and **P<0.01 vs. Control; $^{\#}$P<0.05 and $^{\#\#}$P<0.01 vs. DOX. SSb2, saikosaponin b2; DOX, doxorubicin; H&E, hematoxylin and eosin; MVD, microvessel density.

Results

Effect of SSb2 on tumor growth in H22 tumor-bearing mice. Fig. 1A presented the molecular structure of SSb2. To evaluate its antitumor effect on tumor growth *in vivo*, the tumor weights of H22 tumor-bearing mice treated with 5, 10 or 20 mg/kg SSb2 or DOX for 10 days were assessed. Fig. 1B presented the inhibitory effect of SSb2 on tumor growth, the average tumor weights of the SSb2- and DOX-treated groups were significantly lower compared with those of the control group. The inhibitory rates of tumor growth in the low-, medium- and high-dose SSb2-treated groups and the DOX-treated group were 32.12, 44.85, 55.88 and 62.94%, respectively, which suggested that SSb2 had a concentration-dependent antitumor effect on H22 tumor-bearing mice. Furthermore, the tumor inhibitory rate of high-dose SSb2 did not differ significantly from that of the DOX group.

H&E staining was performed to evaluate pathological changes in the tumors. As presented in Fig. 1D, the control group's tumor cells were heteromorphic and densely arranged, and many obvious nuclear atypia could also be observed in the tumor tissue. However, in the SSb2 and DOX groups, tumor cell growth was disrupted and vacuolated, and the tumor cells displayed a disorganized arrangement and a large, red-stained nucleolytic region. These results demonstrated that SSb2 had a significant antitumor effect on H22 tumor-bearing mice.

Effect of SSb2 on immune function in H22 tumor-bearing mice. To evaluate whether SSb2 administration had any adverse effects on the immune system, the white blood cell count, thymus index and spleen index of the H22 tumor-bearing mice were assessed. As presented in Table I, the white blood cell counts in H22 tumor-bearing mice did not differ significantly between the control,SSb2-treated and DOX-treated groups; however, the thymus and spleen indices in the SSb2-treated mice were significantly lower compared with those in the control group. The thymus and spleen indices of the SSb2-treated mice were, significantly higher compared with those of the DOX group, which indicated that SSb2's immunotoxicity was less severe than that of DOX.

Effect of SSb2 on MVD in H22 tumor-bearing mice. To evaluate whether SSb2 treatment affected angiogenesis in tumor tissues, MVD was assessed using immunohistochemistry with

Table I. Effects of SSb2 on immune function in H22 tumor-bearing mice.

Groups	White blood cell count ($x10^9$/l)	Organ index ($x10^{-3}$)	
		Thymus	Spleen
Control	7.3±3.01	1.80±0.35	6.93±0.62
SSb2, mg/kg			
5	7.3±1.14	1.65±0.30[a,c]	6.61±0.53[d]
10	7.7±1.90	1.54±0.23[a,c]	5.83±0.65[a,c]
20	8.0±1.31	1.16±0.25[b]	5.74±0.55[a,c]
DOX, 2 mg/kg	6.1±2.30	0.93±0.28[b]	4.49±0.57[a]

[a]P<0.05 and [b]P<0.01 vs. Control; [c]P<0.05 and [d]P<0.01 vs. DOX. SSb2, saikosaponin b2; DOX, doxorubicin.

an anti-CD34 antibody. The micrographs in Fig. 1F demonstrated the changes in MVD, where the brown regions indicate angiogenesis. As presented in Fig. 1E, SSb2 or DOX treatment significantly decreased MVD in the tumor tissue. Moreover, SSb2 decreased MVD in a markedly concentration dependent manner, with no significant difference demonstrated between the medium/high-dose SSb2 and DOX groups. These results indicated that SSb2 inhibited angiogenesis in H22 tumor-bearing mice.

Effect of SSb2 on the expression of angiogenesis-related proteins in H22 tumor-bearing mice. To evaluate the mechanisms underlying the suppressive effects of SSb2 on tumor growth, western blotting was used to assess the expression level of proteins involved in the regulation of angiogenesis in tumor tissue. As presented in Fig. 2A-E, the protein expression levels of VEGF, HIF-1α, MMP-2 and MMP-9 markedly decreased in the SSb2-treated groups as the SSb2 concentration increased. As presented in Fig. 2F and G, the concentration-dependent phosphorylation of ERK1/2 was markedly decreased in response to SSb2 treatment; however, the total expression level of ERK1/2 was unaffected. The protein expression levels of VEGF, HIF-1α, MMP-9 and p-ERK1/2 were downregulated in the DOX group. These results suggested that the antitumor mechanism of SSb2 was associated with its antiangiogenic effect via inhibition of the VEGF/ERK/HIF-1α signal pathway.

Effect of SSb2 on HepG2 liver cancer cell viability, migration and expression of angiogenesis-related proteins. HepG2 liver cancer cells were used to investigate the antitumor effect of SSb2 *in vitro*. First, an MTT assay was performed to assess the effect of SSb2 on HepG2 liver cancer cell viability and to determine the nontoxic concentration of SSb2 in the cells. As presented in Fig. 3A, SSb2 significantly inhibited HepG2 liver cancer cell proliferation, in a markedly concentration dependent manner. Based on these results, 15, 30 and 60 μg/ml SSb2 were chosen for use in the following scratch experiment. SSb2 significantly inhibited HepG2 liver cancer cell migration compared with the control group in the scratch wound experiments, as presented in Fig. 3B and C.

To further assess the mechanism underlying the inhibitory effect of SSb2 on HepG2 liver cancer cell proliferation, the protein expression levels of VEGF, HIF-1α, MMP-2 and MMP-9 were analyzed. As presented in Fig. 3D-H, SSb2 at different concentrations significantly inhibited VEGF and HIF-1αprotein expression levels compared with the control. However, MMP2 and MMP9 expression levels were significantly reduced compared with the control, in only the 60 μg/ml SSb2-treated group. The effect of SSb2 on the phosphorylation of ERK1/2 was also assessed; as presented in Fig. 3I and J, protein expression levels of p-ERK1/2 were markedly reduced in different concentrations of the SSb2-treated group, and were significantly reduced compared with the control in the 60 μg/ml SSb2-treated group. These results indicated that SSb2 inhibited the proliferation and migration of HepG2 liver cancer cells, which may be related to its inhibitory effect on the expression of angiogenesis-related proteins in HepG2 liver cancer cells.

Effect of SSb2 on HUVEC viability, migration and invasion. An MTT assay was used to determine the cell viability of HUVECs treated with varying concentrations of SSb2.As shown in Fig. 4A, HUVEC viability significantly decreased compared with the control as the SSb2 concentration increased.

Because the migration of endothelial cells is a critical step in angiogenesis, wound-healing and Transwell assays were performed to evaluate the effect of SSb2 on HUVEC migration. Based on the MTT assay results, 25, 50 and 100 μg/ml SSb2 were selected for use in the subsequent cell migration and invasion experiments. As presented in Fig. 4B and C, after 48 h incubation, HUVECs in the control group had migrated into most of the wound area. However, certain concentrations of SSb2-treated HepG2 significantly decreased the wound-healing capacity in HUVECs compared with the untreated cells. SSb2 also significantly inhibited the migration activity of HUVECs in a concentration-dependent manner, compared with the control, as demonstrated by the Transwell migration assay, presented in Fig. 4D and F, which was used to evaluate the ability of cells to migrate vertically. As presented in Fig. 4E and G, in the Transwell invasion assay, HUVECs demonstrated high levels of invasive activity in the control group. After exposure to SSb2 at 25, 50 or 100 μg/ml, or 5 μg/ml DOX, cell invasion was suppressed by 28.7, 47.1, 74.3, and 71.6%, respectively, which suggested that SSb2 effectively suppressed HUVEC migration and invasion. These results demonstrated the effective *in vitro* antiangiogenic activity of SSb2.

Effect of SSb2 on tube formation as measured using the CAM assay in vivo. A CAM assay was performed to further elucidate the potential function of SSb2 in angiogenesis. SSb2 was injected into the chick embryonic blood vessel branch on incubation day 11 in the presence of b-FGF. As presented in Fig. 5A and B, b-FGF triggered a potent angiogenic response, and the number of branches and vessel diameters of CAM induced by b-FGF were significantly increased compared with the control. Moreover, the 0.1 μg/embryo SSb2 significantly inhibited b-FGF-induced angiogenesis, and SSb2 at concentrations of 0.2 μg/embryo and 0.4 μg/embryo demonstrated greater inhibitory effects on the formation of tube-like vessels,

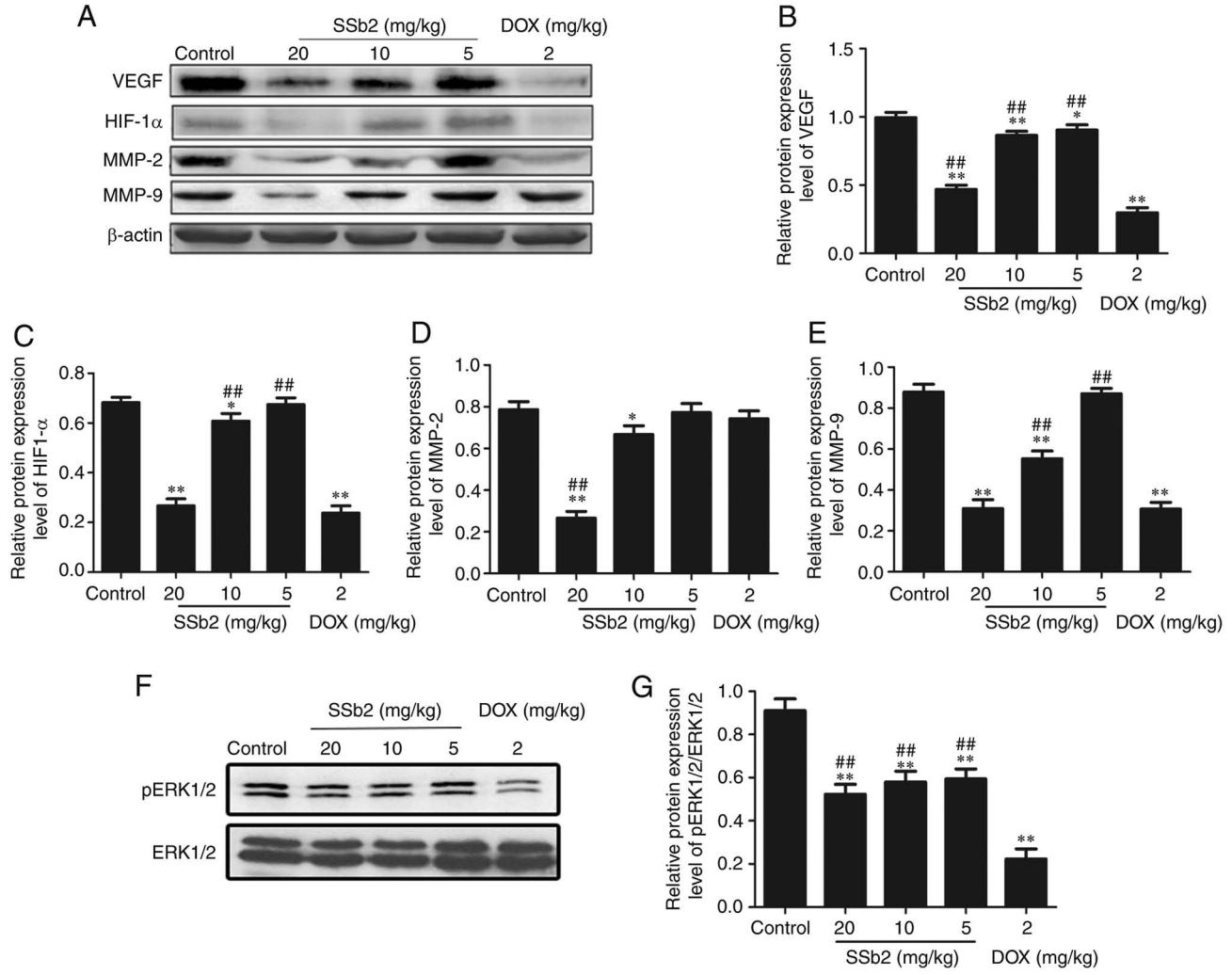

Figure 2. Effects of SSb2 on angiogenesis in tumor tissue of H22 tumor-bearing mice. (A) Representative western blots of VEGF, HIF-1α, MMP-2 and MMP-9. Semi-quantified protein expression levels of (B) VEGF, (C) HIF-1α, (D) MMP-2 and (E) MMP-9. (F) Representative western blots for phosphorylation of ERK1/2 in the tumor tissue of H22 tumor-bearing mice. (G) Semi-quantified protein expression levels of phosphorylation of ERK1/2. β-actin was used as the loading control. Data are presented as mean ± SD. n=3 for each concentration. *P<0.05 and **P<0.01 vs. Control; $^{\#\#}$P<0.01 vs. DOX. HIF-1α, hypoxia-inducible factor-1α; SSb2, saikosaponin b2; DOX, doxorubicin; p, phosphorylated.

which indicated that SSb2 caused a concentration-dependent blockage of the capillary tubes.

Fig. 5C and D presented the inhibitory effect of SSb2 on the CAM model without any inducement. SSb2 and DOX significantly reduced angiogenesis compared with the control, as demonstrated by the induction of fewer vessel branches and a smaller vessel diameter; the effect was amplified at higher SSb2concentrations.These findings suggested that SSb2 was capable of inhibiting angiogenesis *in vivo*.

Discussion

Angiogenesis serves a critical role in solid tumor development by supplying nutrients and oxygen to sustain continuous tumor growth, and numerous malignancies are characterized by intense and rapid angiogenesis. Moreover, angiogenesis is a crucial process in vascular remodeling, tissue damage, tumor migration and invasion (25-27). Therefore, inhibition of tumor angiogenesis is regarded as an effective cancer prevention and treatment strategy. Numerous angiogenesis inhibitors, such as bevacizumab, sunitinib and sorafenib, have been reported to date (28,29). However, recent clinical studies have reported that these antiangiogenic drugs do not have a sufficient curative effect in preventing angiogenesis and tumor development. Furthermore, numerous adverse effects, including hypertension, cardiotoxicity, bleeding, gastrointestinal perforation and birth defects, have been reported during treatment with these drugs (30,31). Therefore, in order to alleviate the suffering of patients and improve their quality of life, more effective and safe angiogenesis drugs must be discovered and developed.

In the present study, the *in vivo* antitumor efficacy of SSb2 was evaluated by assessing the inhibition of tumor growth in H22 tumor-bearing mice. These data showed that SSb2 exhibited remarkable antitumor activity in the H22 tumor-bearing mice model, as a significant concentration-dependent reduction in tumor weight was observed following SSb2 treatment. DOX is a chemotherapeutic drug that is frequently used to treat liver cancer. In the present study, DOX was used as a positive control. These data demonstrated that the tumor-inhibiting

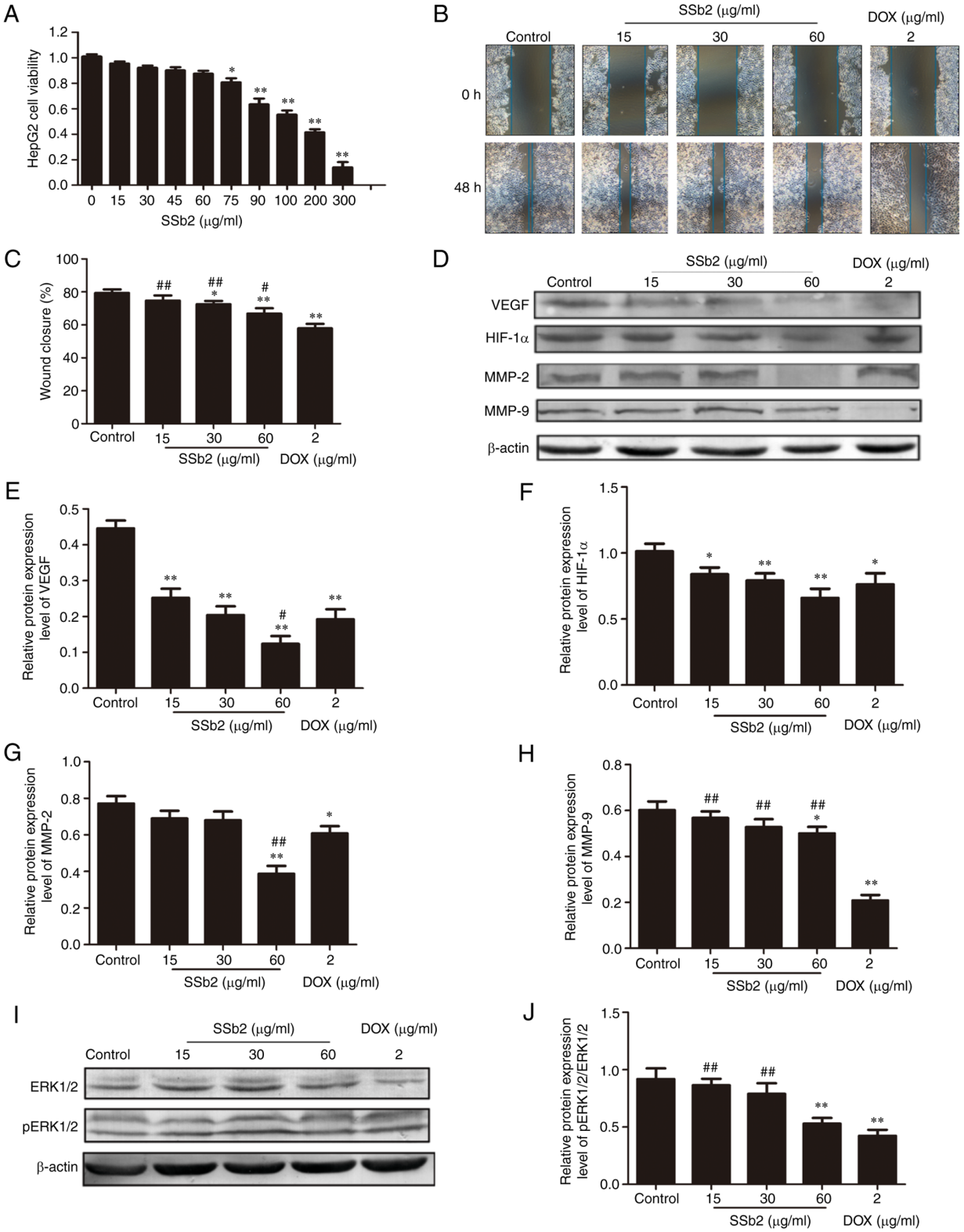

Figure 3. Effects of SSb2 on HepG2 liver cancer cells. (A) The effect of SSb2 on the viability of HepG2 liver cancer cells. (B and C) Effect of SSb2 on the wound-healing ability of HepG2 liver cancer cells (magnification, x100). (D) Representative western blots for VEGF, HIF1-α, MMP-2 and MMP-9 in HepG2 liver cancer cells. β-actin was used as a loading control. Semi-quantified protein expression levels of (E) VEGF, (F) HIF1-α, (G) MMP-2 and (H) MMP-9 in HepG2 liver cancer cells. (I) Representative western blots of the phosphorylation of ERK1/2 in HepG2 liver cancer cells. (J) Semi-quantified protein expression levels of pERK1/2 in HepG2 liver cancer cells. Data are presented as mean ± SD. n=3 for each concentration. *P<0.05 and **P<0.01 vs. Control; $^{\#}$P<0.05 and $^{\#\#}$P<0.01 vs. DOX HIF-1α, hypoxia-inducible factor-1α; SSb2, saikosaponin b2; DOX, doxorubicin; p, phosphorylated.

efficacy of high-dose SSb2 was only marginally inferior to that of DOX. However, the spleen and thymus indices of all SSb2 groups did not decrease as much as those of the DOX group, which indicated that SSb2 induced less immune damage than DOX. Therefore, the antitumor effects of SSb2 were worthy of further study.

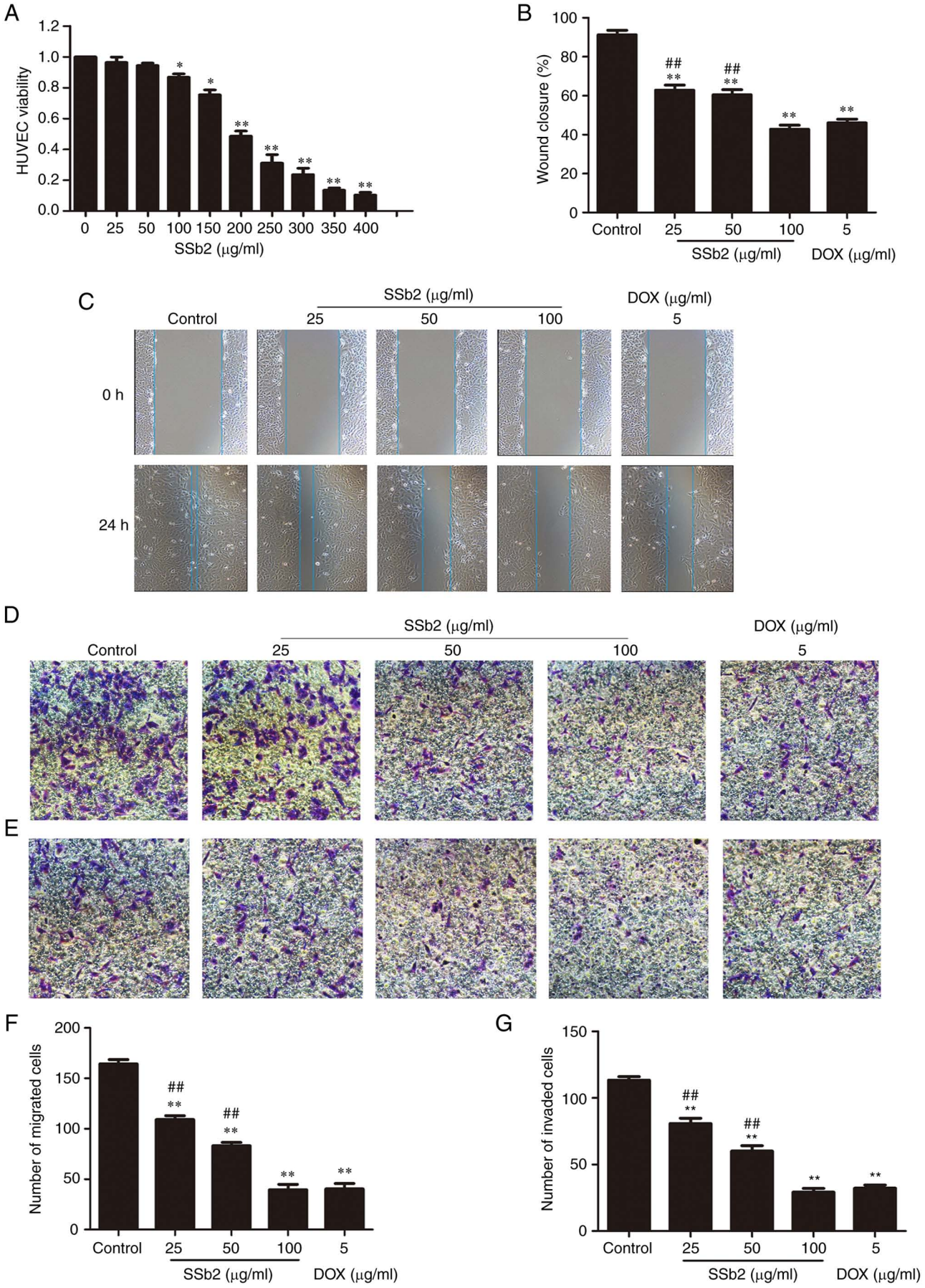

Figure 4. Effects of SSb2 on HUVECs. (A) Effect of SSb2 on the viability of HUVECs. (B and C) Effect of SSb2 on the wound-healing ability of HUVECs (magnification, x100). Effect of SSb2 on the (D and F) migration and (E and G) invasion of HUVECs (magnification, x200). Data are presented as mean ± SD. n=3 for each concentration. *P<0.05 and **P<0.01 vs. Control; $^{\#\#}$P<0.01 vs. DOX. HUVECs, human umbilical vein endothelial cells; SSb2, saikosaponin b2; DOX, doxorubicin.

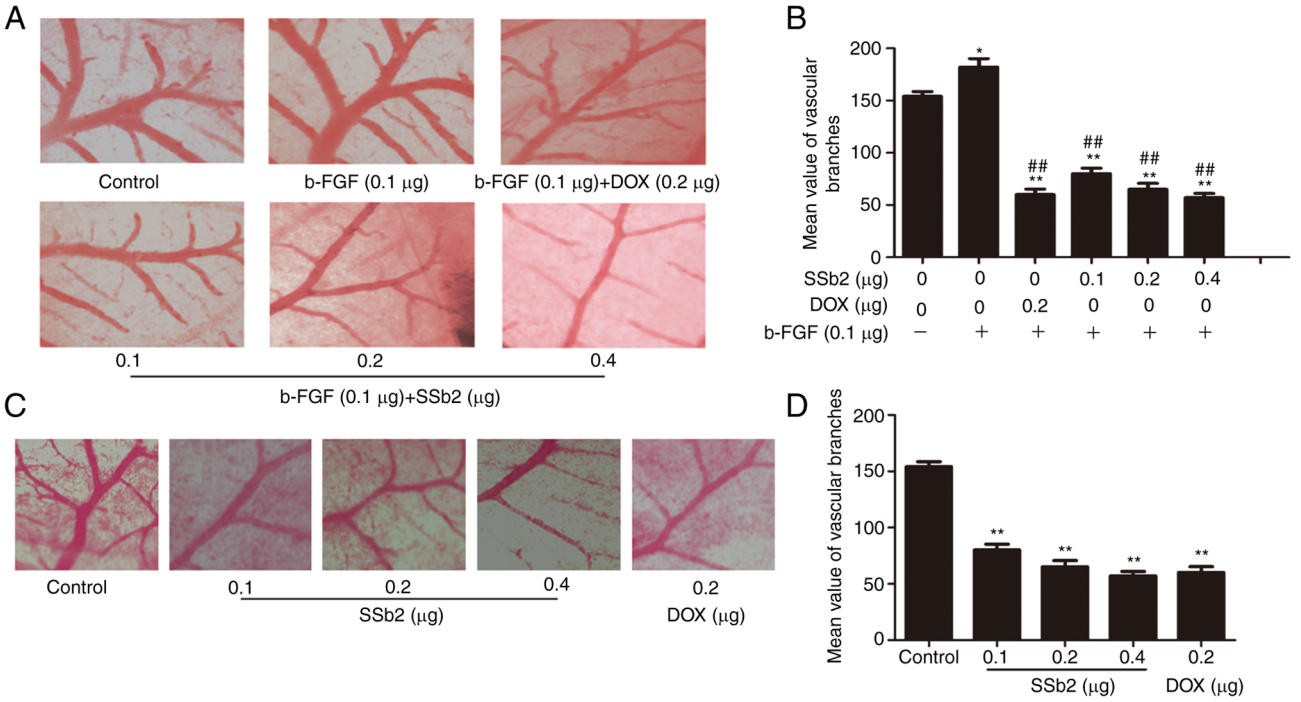

Figure 5. Effects of SSb2 on angiogenesis of CAM. (A) Effect of SSb2 on angiogenesis in an *in vivo* CAM model induced by b-FGF(magnification, x50). (B) Quantification of the number of blood vessels branches after SSb2 treatment in a b-FGF-induced CAM model. (C) The effect of SSb2 on the newly formed blood vessels in the CAM model without induction by b-FGF (magnification, x50). (D) Quantification of the number of branches of new blood vessels after SSb2 treatment in the CAM model. Data are presented as mean ± SD. n=3 for each concentration. *P<0.05 and **P<0.01 vs. Control; $^{\#\#}$P<0.01 vs. DOX. CAM, chorioallantoic membrane; SSb2, saikosaponin b2; DOX, doxorubicin; b-FGF, basic fibroblast growth factor.

MVD is a good indicator of tumor angiogenesis, and the measurement of tumor MVD has become the primary method for determining antiangiogenic drug efficacy (27,32). According to tumor immunohistochemistry, SSb2 markedly decreased the CD34 protein expression level and significantly decreased the corresponding MVD value in tumor tissue, which indicated that SSb2 had antitumor and antiangiogenic activity. These findings were also demonstrated in the CAM model. Due to its advantages of convenient sampling, simple operation, and widespread use, the CAM assay is regarded as a good experimental model for angiogenesis studies and is widely used for screening and evaluating the antiangiogenic activity of drugs (33). As expected, an increase in vessel diameter and branches was observed in the b-FGF control group. However, SSb2 treatment significantly reduced the number of vessel branches and decreased vessel diameter in the CAM model with or without b-FGF. Migration of endothelial cells is an important step in angiogenesis (34). Therefore, HUVECs were used to assess the antiangiogenic effect of SSb2. SSb2 was demonstrated to significantly inhibit both HUVEC migration and invasion. These results validated the antiangiogenic activity of SSb2 both *in vivo* and *in vitro*, which suggested that SSb2 was a potential therapeutic agent for the inhibition of cancer metastasis and tumor angiogenesis. Supporting evidence may provide an experimental basis for further study of SSb2 as a potent angiogenesis inhibitor in clinical applications.

To further investigate the mechanism underlying SSb2's antiangiogenic properties, angiogenesis-related signaling pathways were assessed. VEGF is overexpressed in liver cancer, and its high expression is closely associated with tumor angiogenesis, invasion and metastasis (35,36). VEGF can promote endothelial cell proliferation, increase vascular permeability, enable endothelial cell migration, induce tumor angiogenesis and maintain continued tumor growth by binding and activating VEGFR. As the most powerful angiogenic factor currently known (37), VEGF is related to numerous physiological and pathological processes, including liver cancer development. Any agent inhibiting VEGF-related processes could inhibit angiogenesis and thus restrain tumor growth and metastasis (34). The present study demonstrated that SSb2 inhibited VEGF expression in liver cancer, which suggested that SSb2 suppressed angiogenesis by downregulating VEGF expression, which may be one of the mechanisms by which SSb2 inhibits liver cancer.

The primary characteristic of malignant tumors is their high metastatic potential, which is the primary cause of patient mortality. According to a previous report, >80% of patients with tumors die as a result of tumor metastasis (38). Tumor metastasis is a complex process (39) because many proteolytic enzymes are involved in the degradation of environmental barriers, such as the basal membrane and extracellular matrix, among which MMPs serve an important role in promoting the migration of cancer cells to neighboring tissues by degrading the main components of the basement membrane, such as collagen IV (40,41). Furthermore, HIF-1α acting as a signaling hub can affect the expression of proangiogenic factors, such as VEGF, IL-6 and TNFα (42-45) and proangiogenic enzymes, such as inducible nitric oxide synthase andMMP-9 (43,46,47). VEGF and HIF-1α, which are involved in the regulation of angiogenesis, are deemed the most promising therapeutic targets for direct or indirect angiogenesis inhibitors.

Activation of the MAPK family, including ERK, P38 MAPK and PI3K/Akt, is essential for the promotion of angiogenesis. Therefore, suppression of these pathways may induce anti-angiogenesis and antitumor effects (48-50). The results of the present study demonstrated that SSb2 markedly downregulated the expression of p-ERK1/2, which indicated that SSb2 was capable of modulating ERK1/2 signaling. ERK1/2, a downstream protein of various growth factors, such as VEGF, regulates cell proliferation, differentiation and survival. HIF-1α is a substrate for ERK phosphorylation, and Ser641 and Ser643 phosphorylation of HIF-1α is required for nuclear location and transcriptional activity (51). Zhang *et al* (51) reported that angiogenesis was inhibited by blocking VEGF or downstream molecules such as ERK1/2 and HIF-1α. The present study demonstrated that SSb2 significantly decreased the protein expression levels of VEGF, ERK1/2, HIF-1α, MMP2 and MMP9 compared with the control group. Therefore, we hypothesized that VEGF protein expression levels decreased after SSb2 administration and that VEGF downregulated the expression of ERK1/2, which could inhibit its downstream molecules, including HIF-1α, MMP2 and MMP9. However, HIF-1α can regulate the expression of the VEGF gene, resulting in further VEGF reduction. These effects led to the subsequent inhibition of tumor metastasis and angiogenesis. The present study did not investigate any other pathway activated by VEGF, such as AKT, which is a limitation of the present study and requires study in future research. Furthermore, a gene knockdown or knockout experiment is required to assess the significance of VEGF signaling in SSb2's anticancer activity. Future research must continue to focus on this area.

Overall, the present study demonstrated that SSb2 possesses an antiangiogenic effect both *in vivo* and *in vitro* and that the mechanism appears to involve the inhibition of the VEGF/ERK/HIF-1α signaling pathway. The present study's findings provide new insights into how SSb2 inhibits liver cancer and suggest that SSb2 could be a potential natural product for treating liver cancer. Further studies are needed in to other aspects of SSb2 in the treatment of angiogenesis and cancers.

Acknowledgements

Not applicable.

Funding

This study was supported financially by the Henan Province Key Science and Technology Project (grant no. 202102310486) and Luoyang Science and Technology Medical and Health Project (grant no. 1603001A-3).

Availability of data and materials

The datasets used and/or analyzed during the current study are available from the corresponding author on reasonable request.

Authors' contributions

MY and JF analyzed the data and wrote the manuscript. JF, XL, LW and HW performed the experiments and data collection. RL designed the study and provided the funding and facilities. LW, HW and RL critically reviewed and edited the manuscript. All authors read and approved the final manuscript. JF and RL confirm the authenticity of all the raw data.

Ethics approval and consent to participate

Animal experiment protocols were approved by the Experimental Animal Ethics Committee of Henan University of Science and Technology (approval no. 20200519). All animal experiments were performed in accordance with the National Act on the Use of Experimental Animals (China). Appropriate measures were taken to minimize the use of animals as well as their suffering.

Patient consent for publication

Not applicable.

Competing interests

The authors declare that they have no competing interests.

References

1. Caines A, Selim R and Salgia R: The changing global epidemiology of hepatocellular carcinoma. Clin Liver Dis 24: 535-547, 2020.
2. Liu L, Huang Z, Chen J, Wang J and Wang S: Protein phosphatase 2A mediates JS-K-induced apoptosis by affecting Bcl-2 family proteins in human hepatocellular carcinoma HepG2 cells. J Cell Biochem 119: 6633-6643, 2018.
3. Liu C, Wu J and Chang Z: Trends and age-period-cohort effects on the prevalence, incidence and mortality of hepatocellular carcinoma from 2008 to 2017 in Tianjin, China. Int J Environ Res Public Health 18: 6034, 2021.
4. Qi X, Fan M, Huang N, Zhang XY, Liu J, Li XY and Sun R: Saikosaponin d contributed to cancer chemotherapy induced neutropenia therapy by promoting neutrophil differentiation via activation CBL-dependent ERK pathway. Pharmacol Res 160: 105149, 2020.
5. Chang GR, Lin WL, Lin TC, Liao HJ and Lu YW: The ameliorative effects of saikosaponin in thioacetamide-induced liver injury and non-alcoholic fatty liver disease in mice. Int J Mol Sci 22: 11383, 2021.
6. Liu M, Zhang GF, Naqvi S, Zhang F, Kang T, Duan Q, Wang ZY, Xiao SX and Zheng Y: Cytotoxicity of Saikosaponin A targets HEKa cell through apoptosis induction by ROS accumulation and inflammation suppression via NF-κB pathway. Int Immunopharmacol 86: 106751, 2020.
7. Fang W, Yang YJ, Guo BL and Cen S: Anti-influenza triterpenoidsaponins (saikosaponins) from the roots of Bupleurum marginatum var. stenophyllum. Bioorganic Med Chem Lett 27: 1654-1659, 2017.
8. Li X, Li X, Huang N, Liu R and Sun R: A comprehensive review and perspectives on pharmacology and toxicology of saikosaponins. Phytomedicine 50: 73-87, 2018.
9. You M, Li RF, Gao ZH, Li YY, Liu WY, Wang JG, Wang HW and Li SQ: Effects of saikosaponin b_2 on inflammation and energy metabolism in mice with acute liver injury induced by LPS/GalN. Zhongguo Zhong Yao Za Zhi 44: 2966-2971, 2019 (In Chinese).
10. Wen Y, Zhou X, Lu M, He M, Tian Y, Liu L, Wang M, Tan W, Deng Y, Yang X, *et al*: Bclaf1 promotes angiogenesis by regulating HIF-1α transcription in hepatocellular carcinoma. Oncogene 38: 1845-1859, 2018.
11. Shang R, Song X, Wang P, Zhou Y, Lu X, Wang J, Xu M, Chen X, Utpatel K, Che L, *et al*: Cabozantinib-based combination therapy for the treatment of hepatocellular carcinoma. Gut 70: 1746-1757, 2021.
12. Yao H, Liu N, Lin MC and Zheng J: Positive feedback loop between cancer stem cells and angiogenesis in hepatocellular carcinoma. Cancer Lett 379: 213-219, 2016.
13. Vasudev NS and Reynolds AR: Anti-angiogenic therapy for cancer: Current progress, unresolved questions and future directions. Angiogenesis 17: 471-494, 2014.

14. Tampellini M, Sonetto C and Scagliotti GV: Novel anti-angiogenic therapeutic strategies in colorectal cancer. Exp Opin Investig Drugs 25: 507-520, 2016.
15. Choi SB, Han HJ, Kim WB, Song TJ and Choi SY: VEGF overexpression predicts poor survival in hepatocellular carcinoma. Open Med (Wars) 12: 430-439, 2017.
16. Masoud GN and Li W: HIF-1α pathway: Role, regulation and intervention for cancer therapy. Acta Pharm Sin B 5: 378-389, 2015.
17. Luo D, Wang Z, Wu J, Jiang C and Wu J: The role of hypoxia inducible factor-1 in hepatocellular carcinoma. Biomed Res Int 2014: 409272, 2014.
18. Ju C, Colgan SP and Eltzschig HK: Hypoxia-inducible factors as molecular targets for liver diseases. J Mol Med (Berl) 94: 613-627, 2016.
19. Zhang C, Wang N, Tan HY, Guo W, Chen F, Zhong Z, Man K, Tsao SW, Lao L and Feng Y: Direct inhibition of the TLR4/MyD88 pathway by geniposide suppresses HIF-1α-independent VEGF expression and angiogenesis in hepatocellular carcinoma. Br J Pharmacol 177: 3240-3257, 2020.
20. Liu P, Atkinson SJ, Akbareian SE, Zhou ZG, Munsterberg A, Robinson SD and Bao Y: Sulforaphane exerts anti-angiogenesis effects against hepatocellular carcinoma through inhibition of STAT3/HIF-1α/VEGF signalling. Sci Rep 7: 12651, 2017.
21. Yang HM, Sun CY, Liang JL, Xu LQ, Zhang ZB, Luo DD, Chen HB, Huang YZ, Wang Q, Lee DYW, *et al*: Supercritical-carbon dioxide fluid extract from chrysanthemum indicum enhances anti-tumor effect and reduces toxicity of bleomycin in tumor-bearing mice. Int J Mol Sci 18: 465, 2017.
22. Cao W, Hu C, Wu L, Xu L and Jiang W: Rosmarinic acid inhibits inflammation and angiogenesis of hepatocellular carcinoma by suppression of NF-κB signaling in H22 tumor-bearing mice. J Pharmacol Sci 132: 131-137, 2016.
23. Ting W, Feng C, Zhang M, Long F and Bai M: Overexpression of microRNA-203 suppresses proliferation, invasion, and migration while accelerating apoptosis of CSCC cell line SCL-1. Mol Ther Nucleic Acids 28: 428-440, 2022.
24. Ferreira KCB, Valle ABCDS, Gualberto ACM, Aleixo DT, Silva LM, Santos MM, Costa DS, Oliveira LL, Gameiro J, Tavares GD, *et al*: Kaurenoic acid nanocarriers regulates cytokine production and inhibit breast cancer cell migration. J Control Release 352: 712-725, 2022.
25. Wang L, Liu Y, Li W and Song Z: Growth differentiation factor 15 promotes cell viability, invasion, migration, and angiogenesis in human liver carcinoma cell line HepG2. Clin Res Hepatol Gastroenterol 41: 408-414, 2017.
26. Li S, Xu HX, Wu CT, Wang WQ, Jin W, Gao HL, Li H, Zhang SR, Xu JZ, Qi ZH, *et al*: Angiogenesis in pancreatic cancer: Current research status and clinical implications. Angiogenesis 22: 15-36, 2018.
27. Yang X, Zhang XF, Lu X, Jia HL, Liang L, Dong QZ, Ye QH and Qin LX: MicroRNA-26a suppresses angiogenesis in human hepatocellular carcinoma by targeting hepatocyte growth factor-cMet pathway. Hepatology 59: 1874-1885, 2014.
28. Jung HJ and Kwon HJ: Exploring the role of mitochondrial UQCRB in angiogenesis using small molecules. Mol Biosyst 9: 930-939, 2013.
29. Carmeliet P and Jain RK: Molecular mechanisms and clinical applications of angiogenesis. Nature 473: 298-307, 2011.
30. Chen HX and Cleck JN: Adverse effects of anticancer agents that target the VEGF pathway. Nat Rev Clin Oncol 6: 465-477, 2009.
31. Lim H, Jang JP, Han JM, Jang JH, Ahn JS and Jung HJ: Antiangiogenic potential of microbial metabolite elaiophylin for targeting tumor angiogenesis. Molecules 23: 563, 2018.
32. Lu M, Tian Y, Yue WM, Li L, Li SH, Qi L, Hu WS, Gao C, Si LB and Tian H: GOLPH3, a good prognostic indicator in early-stage NSCLC related to tumor angiogenesis. Asian Pac J Cancer Prev 15: 5793-5798, 2014.
33. Lou C, Zhu Z, Xu X, Zhu R, Sheng Y and Zhao H: Picroside II, an iridoid glycoside from Picrorhizakurroa, suppresses tumor migration, invasion, and angiogenesis in vitro and in vivo. Biomed Pharmacother 120: 109494, 2019.
34. Varinská L, Fáber L, Kello M, Petrovová E, Balážová L, Solár P, Coma M, Urdzík P, Mojžiš J, Švajdlenka E, *et al*: β-Escin effectively modulates HUVECs proliferation and tube formation. Molecules 23: 197, 2018.
35. Carbajo-Pescador S, Ordoñez R, Benet M, Jover R, García-Palomo A, Mauriz JL and González-Gallego J: Inhibition of VEGF expression through blockade of Hif1α and STAT3 signalling mediates the anti-angiogenic effect of melatonin in HepG2 liver cancer cells. Br J Cancer 109: 83-91, 2013.
36. Tseng PL, Tai MH, Huang CC, Wang CC, Lin JW, Hung CH, Chen CH, Wang JH, Lu SN, Lee CM, *et al*: Overexpression of VEGF is associated with positive p53 immunostaining in hepatocellular carcinoma (HCC) and adverse outcome of HCC patients. J Surg Oncol 98: 349-357, 2008.
37. Kämmerer PW, Koch FP, Schiegnitz E, Berres M, Toyoshima T, AI-Nawas B and Brieger J: Associations between single-nucleotide polymorphisms of the VEGF gene and long-term prognosis of oral squamous cell carcinoma. J Oral Pathol Med 42: 374-381, 2013.
38. Kobus-Bianchini K, Bourckhardt GF, Ammar D, Nazari EM and Müller YMR: Homocysteine-induced changes in cell proliferation and differentiation in the chick embryo spinal cord: Implications for mechanisms of neural tube defects (NTD). Reprod Toxicol 69: 167-173, 2017.
39. Bogenrieder T and Herlyn M: Axis of evil: Molecular mechanisms of cancer metastasis. Oncogene 22: 6524-6536, 2003.
40. Deng G, Zhou F, Wu Z, Zhang F, Niu K, Kang YJ, Liu XJ, Wang QJ, Wang Y and Wang Q: Inhibition of cancer cell migration with CuS@mSiO$_2$-PEG nanoparticles by repressing MMP-2/MMP-9 expression. Int J Nanomedicine 13: 103-116, 2017.
41. Zou Y, Xiong H, Xiong H, Lu T, Zhu F, Luo Z, Yuan X and Wang Y: A polysaccharide from mushroom Huaier retards human hepatocellular carcinoma growth, angiogenesis, and metastasis in nude mice. Tumor Biol 36: 2929-2936, 2014.
42. Medrek C, Pontén F, Jirström K and Leandersson K: The presence of tumor associated macrophages in tumor stroma as a prognostic marker for breast cancer patients. BMC Cancer 12: 306, 2012.
43. Werno C, Menrad H, Weigert A, Dehne N, Goerdt S, Schledzewski K, Kzhyshkowska J and Brune B: Knockout of HIF-1α in tumor-associated macrophages enhances M2 polarization and attenuates their pro-angiogenic responses. Carcinogenesis 31: 1863-1872, 2010.
44. Yang XM, Wang YS, Zhang J, Li Y, Xu JF, Zhu J, Zhao W, Chu DK and Wiedemann P: Role of PI3K/Akt and MEK/ERK in mediating hypoxia-induced expression of HIF-1α and VEGF in laser-induced rat choroidal neovascularization. Invest Opthalmol Visual Sci 50: 1873-1879, 2009.
45. Coffelt SB, Tal AO, Scholz A, Palma MD, Patel S, Urbich C, Biswas SK, Murdoch C, Plate KH, Reiss Y and Lewis CE: Angiopoietin-2 regulates gene expression in TIE2-expressing monocytes and augments their inherent proangiogenic functions. Cancer Res 70: 5270-5280, 2010.
46. Du R, Lu KV, Petritsch C, Liu P, Ganss R, Passegué E, Song H, VandenBerg S, Johnson RS and Werb Z: HIF1α induces the recruitment of bone marrow-derived vascular modulatory cells to regulate tumor angiogenesis and invasion. Cancer Cell 13: 206-220, 2008.
47. Chen WT, Hung WC, Kang WY, Huang YC, Su YC, Yang CH and Chai CY: Overexpression of cyclooxygenase-2 in urothelial carcinoma in conjunction with tumor-associated-macrophage infiltration, hypoxia-inducible factor-1α expression, and tumor angiogenesis. APMIS 117: 176-184, 2009.
48. Herrera-Vargas AK, García-Rodríguez E, Olea-Flores M, Mendoza-Catalán MA, Flores-Alfaro E and Navarro-Tito N: Pro-angiogenic activity and vasculogenic mimicry in the tumor microenvironment by leptin in cancer. Cytokine Growth Factor Rev 62: 23-41, 2021.
49. Baek SH, Ko JH, Lee JH, Kim C, Lee H, Nam D, Lee J, Lee SG, Yang WM, Um JY, *et al*: Ginkgolic acid inhibits invasion and migration and TGF-β-induced EMT of lung cancer cells through PI3K/Akt/mTOR inactivation. J Cell Physiol 232: 346-354, 2017.
50. Singh SS, Yap WN, Arfuso F, Kar S, Wang C, Cai W, Dharmarajan AM, Sethi G and Kumar AP: Targeting the PI3K/Akt signaling pathway in gastric carcinoma: A reality for personalized medicine? World J Gastroenterol 21: 12261-12273, 2015.
51. Zhang Y, Jiang X, Qin X, Ye D, Yi Z, Liu M, Bai O, Liu W, Xie X, Wang Z, *et al*: RKTG inhibits angiogenesis by suppressing MAPK-mediated autocrine VEGF signaling and is downregulated in clear-cell renal cell carcinoma. Oncogene 29: 5404-5415, 2010.